Computational Mechanics, 27 (2001) 188-198, Springer-Verlag

A Meshless Local Petrov-Galerkin (MLPG) method for free and forced vibration analyses for solids

Y. T. Gu and G. R. Liu*
Dept. of Mechanical Engineering
National University of Singapore
10 Kent Ridge Crescent, Singapore 119260

Abstract

The Meshless Local Petrov-Galerkin (MLPG) method is an effective truly meshless method for solving partial differential equations using Moving Least Squares (MLS) interpolants and local weak forms. In this paper, a MLPG formulation is proposed for free and forced vibration analyses. Local weak forms are developed using weighted residual method locally from the dynamic partial differential equation. In the free vibration analysis, the essential boundary conditions are implemented through the direct interpolation form and imposed using orthogonal transformation techniques. In the forced vibration analysis, the penalty method is used in implementation essential boundary conditions. Two different time integration methods are used and compared in the forced vibration analyses using the present MLPG method. The validity and efficiency of the present MLPG method are demonstrated through a number of examples of two-dimensional solids.

KEY WORDS: Meshless Method; Meshless Local-Galerkin Method; Free Vibration; Forced Vibration; Numerical Analysis

---

* Correspondence to: Gui-Rong LIU
E-mail: mpeliugr@nus.edu.sg, engp8973@nus.edu.sg

1. Introduction

The vibration analysis for structures is a very important field in computational mechanics. These dynamic problems are classically described by a linear partial differential equation associated with a set of boundary conditions and initial conditions. Exact analyses of these dynamic problems are usually very difficult. Analytical solutions to these boundary value and initial value problems are only in relatively few cases (Meirovitch, 1980). Therefore, numerical techniques with different discretization schemes, such as Finite Element Method (FEM), are widely used in these analyses.

Meshless methods have become recently attractive alternatives for problems in computational mechanics, as it does not require a mesh to discretize the problem domain, and the approximate solution is constructed entirely based on a set of scattered nodes. Meshless methods may be largely divided into two categories: domain type methods and boundary type methods. In these two types meshless methods, the problem domain or only the boundary of the problem domain is discretized by properly scattered nodes. Several domain type meshless methods, such as, Diffuse Element Method (DEM) (Nayroles et al., 1992), Element Free Galerkin (EFG) method (Belytschko et al, 1994), Reproducing Kernel Particle Method (RKPM) (Liu et al, 1995), Point Interpolation Method (PIM) (Liu and Gu, 2001), Point Assembly Method (PAM)(Liu,1999) have been proposed and achieved remarkable progress in solving a wide range of static and dynamic problems. The boundary type meshless methods proposed include Boundary Node Method (BNM) (Mukherjee and Mukherjee, 1997; Chati and Mukherjee,2000) and Boundary Point Interpolation Method (BPIM) (Gu and Liu, 2000a). In addition, techniques of coupling meshless methods with other established numerical methods have

also been proposed, such as coupled EFG/FEM (Belytschko and Organ, 1995), EFG/Boundary Element Method (BEM) (Gu and Liu, 2000b; Liu and Gu, 2000a).

In particular, the above-mentioned meshless methods are "meshless" only in terms of the interpolation of the field or boundary variables, as compared to the usual Finite Element Method (FEM) or Boundary Element Method (BEM). Most of meshless methods have to use background cells to integrate a weak form over the problem domain or boundary. The requirement of background cells for integration makes the method being not "truly" meshless.

Three truly meshless methods, called the Meshless Local Petrov-Galerkin (MLPG) method, the Local Boundary Integral Equation (LBIE) method, and the Local Point Interpolation Method (LPIM), have been developed by Atluri and Zhu (1998,2000a,b), Atluri et al. (1999a,b), Zhu et al. (1998), Liu and Gu (2000b). The MLPG method is based on a local weak form and Moving Least Squares (MLS) approximation. In the MLPG, an integration method in a regular-shaped local domain (such as spheres, rectangular, and ellipsoids) is used. The MLPG method does not need any "element" or "mesh" for both field interpolation and background integration. Therefore, it is a "truly" meshless method. Up to now, the MLPG method has been formulated only in static analyses of solids. For example, the MLPG method has been used for two-dimensional elasto-statics (Atluri and Zhu 2000b) and one-dimensional 4th order thin beam static analysis (Atluri et al. 1999a). Very good results have been obtained.

However, it is difficult to implement essential boundary conditions in MLPG, because shape functions, which constructed by MLS approximation, lack the delta function property. Some special techniques have to be used to overcome above-mentioned

problems in using MLPG to static analyses. For example, the Lagrange multiplier method, the penalty method (Atluri and Zhu 2000a), the orthogonal transformation technique (Atluri et al. 1999b; Ouatouati and Johnson, 1999), and the direct interpolation method (Liu and Yan 2000) have been used to deal with essential boundary conditions.

MLPG formulations for free vibration and forced vibration analyses of two-dimensional solids and structures are proposed in this paper to extend the MLPG method to dynamic analyses. Local weak forms are developed using weighted residual method locally from the dynamic partial differential equation. The MLS approximation is used to obtain the shape functions. In free vibration analysis, the essential boundary conditions are formulated separately through a direct interpolation form. The boundary conditions are then imposed utilizing orthogonal transform techniques to eliminate the independent modes. Frequencies and eigenmodes of free vibration are obtained by solving an eigenvalue equation. In the forced vibration analysis, the penalty method is used to implement the essential conditions. Both explicit time integration method (the central difference method) and implicit time integration method (the Newmark method) are used to solve the forced vibration system equations.

Programs of the MLPG method have been developed in FORTRAN, and a number of numerical examples of free vibration and forced vibration analyses are presented to demonstrate the convergence, validity and efficiency of the present methods. Some important parameters on the performance of the present method are also investigated thoroughly in this paper.

2. Moving Least Square (MLS) approximation

In this section a briefing of MLS approximation is given. More details can be found in a paper by Lancaster and Salkauskas (1981) .

Consider a problem domain Ω. To approximate a function $u(\mathbf{x})$ in Ω, a finite set of $\mathbf{p}(\mathbf{x})$ called basis functions is considered in the space coordinates $\mathbf{x}^{\mathrm{T}}=[x, y]$. The basis functions in two-dimension is given by

$$\mathbf{p}^{\mathrm{T}}(\mathbf{x})=[1, x, y, x^2, xy, y^2 \ldots] \tag{1}$$

The MLS interpolant $u^h(x)$ is defined in the domain Ω by

$$u^h(\mathbf{x}) = \sum_{j=1}^{m} p_j(\mathbf{x}) a_j(\mathbf{x}) = \mathbf{p}^{\mathrm{T}}(\mathbf{x})\mathbf{a}(\mathbf{x}) \tag{2}$$

where m is the number of basis functions, the coefficient $a_j(x)$ in equation (2) is also functions of $\mathbf{x}$; $\mathbf{a}(\mathbf{x})$ is obtained at any point $\mathbf{x}$ by minimizing a weighted discrete $\mathbf{L}_2$ norm of:

$$J = \sum_{i=1}^{n} \upsilon(\mathbf{x} - \mathbf{x}_i)[\mathbf{p}^{\mathrm{T}}(\mathbf{x}_i)\mathbf{a}(\mathbf{x}) - u_i]^2 \tag{3}$$

where n is the number of points in the neighborhood of $\mathbf{x}$ for which the weight function $\upsilon(\mathbf{x}\text{-}\mathbf{x}_i)\neq 0$, and u_i is the nodal value of u at $\mathbf{x}=\mathbf{x}_i$.

The stationarity of J with respect to $\mathbf{a}(\mathbf{x})$ leads to the following linear relation between $\mathbf{a}(\mathbf{x})$ and u_i:

$$\mathbf{A}(\mathbf{x})\mathbf{a}(\mathbf{x})=\mathbf{B}(\mathbf{x})\mathbf{u} \tag{4}$$

Solving $\mathbf{a}(\mathbf{x})$ from equation (4) and substituting it into equation (2), we have

$$u^h(\mathbf{x}) = \sum_{i=1}^{n} \phi_i(\mathbf{x}) u_i \tag{5}$$

where the MLS shape function $\phi_i(\mathbf{x})$ is defined by

$$\phi_i(\mathbf{x}) = \sum_{j=1}^{m} p_j(\mathbf{x})(\mathbf{A}^{-1}(\mathbf{x})\mathbf{B}(\mathbf{x}))_{ji} \tag{6}$$

where $\mathbf{A}(\mathbf{x})$ and $\mathbf{B}(\mathbf{x})$ are the matrices defined by

$$\mathbf{A}(\mathbf{x}) = \sum_{i=1}^{n} \upsilon_i(\mathbf{x})\mathbf{p}^{\mathrm{T}}(\mathbf{x}_i)\mathbf{p}(\mathbf{x}_i), \quad \upsilon_i(\mathbf{x}) = \upsilon(\mathbf{x}-\mathbf{x}_i) \tag{7}$$

$$\mathbf{B}(\mathbf{x}) = [\upsilon_1(\mathbf{x})\mathbf{p}(\mathbf{x}_1), \upsilon_2(\mathbf{x})\mathbf{p}(\mathbf{x}_2), \ldots, \upsilon_n(\mathbf{x})\mathbf{p}(\mathbf{x}_n)] \tag{8}$$

It can be found from above discussion that the MLS approximation does not pass through the nodal parameter values. Therefore the MLS shape functions given in equation (6) do not, in general, satisfy the Kronecker delta condition. Thus,

$$\phi_i(\mathbf{x}_j) \neq \delta_{ij} = \begin{cases} 1 & i = j \\ 0 & i \neq j \end{cases} \tag{9}$$

The choice of weight function plays an important role in the performance of the MLS interpolation. Many kinds of weight functions can be chosen (Belytscko et al.,1994). In this paper, the following 4-orders spline function is used:

$$\upsilon_i(x) = \begin{cases} 1 - 6\left(\dfrac{d_i}{r_\upsilon}\right)^2 + 8\left(\dfrac{d_i}{r_\upsilon}\right)^3 - 3\left(\dfrac{d_i}{r_\upsilon}\right)^4 & 0 \le d_i \le r_\upsilon \\ 0 & d_i \ge r_\upsilon \end{cases} \tag{10}$$

Where $d_i = |\mathbf{x}_Q - \mathbf{x}_i|$ is the distance from node $\mathbf{x}_i$ to the sampling point $\mathbf{x}_Q$, r_υ is the size of the support for the weight function.

In MLS approximation, the number of nodes, n, chosen in the influence domain should ensure matrix **A** in equation (6) invertible and the interpolation accurate. The reasonable n depends on the problem and the number of basis function, m. It has been found (Chati and Mukherjee, 2000) that n~15-30 leads to acceptable results for 2-D problem and m~3-6.

3.Basic equations of elastodynamics

The strong form of the initial/boundary value problem for small displacement elastodynamics is as follows:

$$\sigma_{ij,j} + b_i = m\ddot{u}_i + c\dot{u}_i \tag{11}$$

where m is the mass density, c is the damping coefficient, $\ddot{u}_i = \frac{\partial^2 u_i}{\partial t^2}$ is the acceleration, $\dot{u}_i = \frac{\partial u_i}{\partial t}$ the velocity, σ_{ij} the stress tensor, which corresponds to the displacement field u_i, b_i the body force tensor, and $(\,)_{,j}$ denotes $\frac{\partial}{\partial x_j}$. The auxiliary conditions are given as follows:

Natural boundary condition: $\sigma_{ij} n_j = \bar{t}_i$ on Γ_t (12a)

Essential boundary condition: $u_i = \bar{u}_i$ on Γ_u (12b)

Displacement initial condition: $\mathbf{u}(\mathbf{x}, t_0) = \mathbf{u}_0(\mathbf{x})$ $\mathbf{x} \in \Omega$ (12c)

Velocity initial condition: $\dot{\mathbf{u}}(\mathbf{x}, t_0) = \mathbf{v}_0(\mathbf{x})$ $\mathbf{x} \in \Omega$ (12d)

in which the $\bar{u}_i$, $\bar{t}_i$, $\mathbf{u}_0$ and $\mathbf{v}_0$ denote the prescribed displacements, tractions, initial displacements and velocities, respectively, and n_j is the unit outward normal to domain Ω.

4. Free vibration analysis

4.1 Local weak form

The governing equation for no damping free vibration is as follows:

$$\sigma_{ij,j} = m\ddot{u}_i \tag{13}$$

The boundary conditions are usually the same form of equations (12a) and (12b), but the traction $\bar{t} = 0$. In the free vibration analysis, $\mathbf{u}(\mathbf{x},t)$ can be written as

$$\mathbf{u}(\mathbf{x},t) = \mathbf{u}(\mathbf{x})\sin(\omega t + \varphi) \tag{14}$$

where ω is the frequency. Substituting equation (14) into equation (13) leads to the following equations

$$\sigma_{ij,j} + \omega^2 m u_i = 0 \tag{15}$$

It should be noted that the stresses, $\boldsymbol{\sigma}$, and displacements, $\mathbf{u}$, in equation (15) are only the function of coordinator $\mathbf{x}$.

A local weak form of equation (15), over a local sub-domain Ω_s bounded by Γ_s, can be obtained using the weighted residual method

$$\int_{\Omega_s} w_i(\sigma_{ij,j} + \omega^2 m u_i)\mathrm{d}\Omega = 0 \tag{16}$$

where w_i is the weight function.

The first term on the left hand side of equation (16) can be integrated by parts to become

$$\int_{\Gamma_s} w_i \sigma_{ij} n_j \mathrm{d}\Gamma - \int_{\Omega_s} (w_{i,j}\sigma_{ij} - w_i \omega^2 m u_i)\mathrm{d}\Omega = 0 \tag{17}$$

The support sub-domain Ω_s of a node $\mathbf{x}_i$ is a domain in which $w_i(x)\neq 0$. A arbitrary shape support domain can be used (Atluri et al 1999b). A circle or rectangular support domain is used in this paper for convenience. From Figure 1, it can be found that the boundary Γ_s for the support domain Ω_s is usually composed by three parts: the internal boundary Γ_{si}, the boundaries Γ_{su} and Γ_{st}, over which the essential and natural boundary conditions are specified. Imposing the natural boundary condition and noticing that $\sigma_{ij} n_j = \dfrac{\partial u}{\partial n} \equiv t_i$ in equation (17), we obtain:

$$\int_{\Gamma_{si}} w_i t_i \mathrm{d}\Gamma + \int_{\Gamma_{su}} w_i t_i \mathrm{d}\Gamma + \int_{\Gamma_{st}} w_i \bar{t}_i \mathrm{d}\Gamma - \int_{\Omega_s} (w_{i,j}\sigma_{ij} - w_i \omega^2 m u_i)\mathrm{d}\Omega = 0 \tag{18}$$

For a support domain located entirely within the global domain, there is no intersection between Γ_s and the global boundary Γ, $\Gamma_{si}=\Gamma_s$, and the integrals over Γ_{su} and Γ_{st} vanish. Because of $\bar{t}=0$ on Γ_t, the integrals over Γ_{st} vanish for all nodes in the free vibration analysis.

With equation (18) for any node $\mathbf{x}_i$, instead of dealing with a global problem equation (15), the problem becomes to deal with a localized problem over a local support domain.

The problem domain Ω is represented by properly scattered nodes. The MLS approximation (5) is used to approximate the value of a point $\mathbf{x}_Q$. Substituting equation (5) into the local weak form (18) for all nodes leads to the following discrete system equations

$$\mathbf{Ku}-\omega^2\mathbf{Mu}=0 \tag{19}$$

where the "stiffness" matrix **K** and "mass" matrix **M** are defined by

$$\mathbf{K}_{(\mathrm{MLPG})ij}=\int_{\Omega_s}\mathbf{v}_i{}^{\mathrm{T}}\mathbf{DB}_j\mathrm{d}\Omega-\int_{\Gamma_{si}}\mathbf{w}_i\mathbf{NDB}_j\mathrm{d}\Gamma-\int_{\Gamma_{su}}\mathbf{w}_i\mathbf{NDB}_j\mathrm{d}\Gamma \tag{20a}$$

$$\mathbf{M}_{ij}=\int_{\Omega_s}m\mathbf{w}_i\mathbf{\Phi}_j\mathrm{d}\Omega \tag{20b}$$

with **w** being the value of the weight function matrix, $\mathbf{\Phi}$ being the shape function matrix, corresponding to node *i*, evaluated at the point **x**, and

$$\mathbf{N}=\begin{bmatrix} n_x & 0 & n_y \\ 0 & n_y & n_x \end{bmatrix} \tag{20c}$$

$$\mathbf{B}_j=\begin{bmatrix} \phi_{j,x} & 0 \\ 0 & \phi_{j,y} \\ \phi_{j,y} & \phi_{j,x} \end{bmatrix} \tag{20d}$$

$$\mathbf{v}_i = \begin{bmatrix} w_{i,x} & 0 \\ 0 & w_{i,y} \\ w_{i,y} & w_{i,x} \end{bmatrix} \tag{20e}$$

$$\mathbf{D} = \begin{bmatrix} 1 & \upsilon & 0 \\ \upsilon & 1 & 0 \\ 0 & 0 & (1-\upsilon)/2 \end{bmatrix} \quad \text{for plane stress} \tag{20f}$$

For free vibration analyses, equation (19) can also be written as:

$$(\mathbf{K} - \omega^2 \mathbf{M})\mathbf{q} = 0 \tag{21}$$

where **q** is the eigenvector. Equation (21) is the MLPG local weak formulation for free vibration analysis. In order to determine the frequencies, ω, and free vibration modes, it is necessary to solve the linear eigenvalue equation. However, It remains the essential boundary condition equation (12b) need be satisfied.

4.3 Imposition of essential boundary conditions

In the MLPG method, it is difficult to implement essential boundary conditions, because the shape functions constructed by MLS approximation lack the delta function property. In static analyses, strategies have been developed for alleviating the above problem, such as using the Lagrange multiplier method, the penalty method (Atluri and Zhu, 1998), and the direct interpolation method (Liu and Yan, 2000). In free vibration analyses using the MLPG method, orthogonal transform techniques (Atluri et al., 1999b; Ouatouati and Johnson, 1999) are utilized in order to eliminate the independent modes.

For free vibration analysis, the essential boundary conditions are always homogeneous, therefore, we have $\bar{u}_i = 0$ in equation (12b). Substituting equation (5) into the equation (12b), we find a set of algebraic linear constraint equations

$$\mathbf{C}\mathbf{q} = 0 \tag{22}$$

Using singular value decomposition (Strang, 1976), **C** can be decomposed as:

$$\mathbf{C} = \mathbf{U}\sum\mathbf{V}^{\mathrm{T}} \tag{23}$$

where **U** and **V** are orthogonal matrices, **Σ** has diagonal form which diagonal elements are equal to singular values of **C**. The matrix **V** can be written as:

$$\mathbf{V}^{T} = \left\{\mathbf{V}_{n\times r}, \mathbf{V}_{n\times(n-r)}\right\}^{\mathrm{T}} \tag{24}$$

where *r* is the rank of **C**, namely the number of independent constraints.

Performing coordinate transformation:

$$\mathbf{q} = \mathbf{V}_{n\times(n-r)}\tilde{\mathbf{q}} \tag{25}$$

The change of co-ordinates satisfies the constrain equation (22). Substituting equation (25) into equation (21), leads to:

$$(\tilde{\mathbf{K}} - \boldsymbol{\omega}^2\tilde{\mathbf{M}})\tilde{\mathbf{q}} = \mathbf{0} \tag{26}$$

where $\tilde{\mathbf{K}}_{(n-r)\times(n-r)} = \mathbf{V}^{T}_{(n-r)\times n}\mathbf{K}_{n\times n}\mathbf{V}_{n\times(n-r)}$ and $\tilde{\mathbf{M}}_{(n-r)\times(n-r)} = \mathbf{V}^{T}_{(n-r)\times n}\mathbf{M}_{n\times n}\mathbf{V}_{n\times(n-r)}$ are the dimension reduced stiffness and mass matrices. After the above discussed orthogonal transform, essential boundary conditions have been satisfied and independent modes have been eliminated in equation (26).

4.3 Numerical implementation of the MLPG method

Theoretically, as long as the union of all local domains, Ω_s, covers the global domain Ω, the equilibrium equation and the boundary conditions will be satisfied in the global domain Ω and in its boundary Γ by using above discussed MLPG formulation. However, the support domain used will affect the solution, especially in dynamic analyses. The

influence on of the choice of local support domain will be studied in the following numerical examples.

As the MLPG is regarded as a weighted residual method, the weight function plays an important role in the performance of the method. Theoretically, as long as the condition of continuity is satisfied, any weight function is acceptable. However, the local weak form is based on the local sub-domains centered by nodes. It can be found that the weight function with the local property, which should decrease in magnitude as the distance from a point $\mathbf{x}_Q$ to the node $\mathbf{x}_i$ increases, yields better results. Therefore, we will consider weight functions, which only depend on the distance between two points, such as the spline weight functions equation (10). It can be easily seen that the system stiffness matrix **K** in the present method is banded but usually asymmetric. However, similarly as Galerkin FE methods, the weight function, w, can be take as the same formulation as equation (5). In this case **K** becomes symmetrical (Atluri et al., 1999b). This symmetrical stiffness matrix can be an added advantage in applying the present MLPG method.

A numerical integration is needed to evaluate the integration in equation (20). The Gauss quadrature is used in the MLPG method. For a node $\mathbf{x}_i$, a local integration cell is needed to employ Gauss quadrature. For each Gauss quadrature point $\mathbf{x}_Q$, the MLS interpolation is performed to obtain the integrand. Therefore, as shown in Figure 1, for a node $\mathbf{x}_i$, there exist three local domains: local integration domain Ω_Q (size r_q), weight function domain Ω_w (same as Ω_s) for $w_i \neq 0$ (size r_w), and interpolation domain Ω_i for x_Q (size r_i). These three local domains are independent as long as the condition $r_q \leq r_w$ is satisfied. It should be noted that when the weight function is used in the form of equation (10), the weight function w will be zero along the boundary of integration domain if the

integration domain and weight domain are same(r_q=r_w). Hence, the equation (20b) can be simplified because the integration along the internal boundary Γ_{si} vanishes. Because the problem domains in following examples are rectangle domains, rectangle sub-domains are used for establishing weight function. The size of the sub-domain for node *i* is defined

$$r_w=\alpha d_i \tag{27}$$

where, α is a coefficient chosen. The d_i is the shortest distance between the node *i* and neighbor nodes. It has been found in the static analyses that α=1.0~3.0 can obtain an acceptable result (Liu and Yan 2000).

There exit difficulties to obtain the exact numerical integration in meshless methods (Atluri et al., 1999b; Dollow and Belytschko, 1994; Liu and Yan, 1999). Insufficiently accurate numerical integration may cause a deterioration and a rank-deficiency in the numerical solution. The numerical integration errors are results from the complexities of the integrand. First, the shape functions constructed using the MLS approximation have a complex feature. The shape functions have different form in each small integration region. The derivatives of shape functions might have an oscillation. Second, the overlapping of interpolation domains makes the integrand in the overlapping domain is very complicated. In order to guarantee the accuracy of the numerical integration, the Ω_Q should be divided into small regular partitions. In each small partition, more Gauss quadrature points should be used (Atluri et al. 1999b).

4.4 Numerical results

The MLPG method is used for free vibration analysis of 2-D structures. Except special mentioned, the units are taken as standard international (SI) units in following examples**.**

Example 1: A cantilever beam

The MLPG method is applied to analyze free vibration of a cantilever beam as shown in Figure 2. The problem has been analyzed by Nagashima (1999) using Node-By-Node Meshless (NBNM) method. A plane stress problem is considered. The parameters are taken as length L=100mm, height D=10mm, thickness t=1.0mm, Young's modulus E=2.1×10^{4}kgf/mm^2, Poisson ration ν=0.3, mass density m=8.0×10^{-10} kgfs^2/mm^4. Figure 3 shows two kinds of nodal arrangements, coarse (63 nodes) arrangement and fine arrangement (306 nodes). Different sizes of sub-domains are investigated with different α in equation (27). It can be found that α=1.5~2.5 can obtain almost identical results in the free vibration analyses. Therefore, α=1.5 is used in following free vibration analyses. Frequency results of these two nodal arrangements obtained by MLPG are listed in Table 1. The results obtained by FEM software, ABAQUS, and NBNM method (Nagashima, 1999) are listed in the same table. From this table, one can observe that the results by the present MLPG method is in good agreement with those obtained using FE and NBNM methods. The convergence of the present method is also demonstrated in this table. As the number of nodes increases, results obtained by the present MLPG approach to the FEM results (if we consider the FEM results as a reference). The first ten eigenmodes obtained by MLPG method are plotted in Figure 4. Comparing with FEM results and Nagashima's(1999) results, almost identical results are obtained.

In Timoshenko beam theory, the slenderness of a beam is expressed by the slenderness ratio, r/L, where $r=\sqrt{I/A}$ is the radius of gyration of the cross-section, I the moment of inertia, and L the length of the beam. Beams with two slenderness ratios, r/L=0.029(L=100,D=10,t=1.0) and 0.144(L=100,D=50,t=1.0), are analyzed. The

frequency results are list in table 2. Comparing with the Euler-Bernoulli beam results, as the slenderness ratio r/L decreases, it can be found that the natural frequencies of this two-dimensional beam approach the values for an Euler-Bernoulli model.

Example 2: A variable cross-section beam

In this example the present MLPG method is used in free vibration analysis of cantilever beam with variable cross-section, shown in Figure 5. Results are obtained for following numerical parameters: the length L=10, the height $h(0)$=5, $h(L)$=3, the thickness t=1.0, E =3.0×10^7, ν=0.3 and m=1.0. The nodal arrangement is shown in Figure 5. Results obtained by the presented MLPG method and the FEM software, ABAQUS, are listed and compared in Table 3. Results obtained by these two methods are in very good agreement.

Example 3: A shear wall

Figure 6 shows a shear wall with four openings, which has been solved using Boundary Element Method by some researchers (Brebbia et al., 1984). The problem is solved for the plane stress case with E=1000, ν=0.2,t=1.0 and m=1.0. 574 uniformed nodes are used to discretize the problem domain. The problem is also analyzed by FEM software ABAQUS. Natural frequencies of the first 8 modes are calculated and listed in Table 4. Results obtained by BEM and FEM are listed in the same table. Results obtained by the present MLPG method are in very good agreement with those obtained using BEM and FEM.

5. Forced vibration analysis

5.1 Local weak form

The governing equation for forced vibration of 2-D solids is equation (11). The boundary conditions and initial conditions are given in equation (12). The penalty method

is used to enforce the essential boundary conditions. A local weak form of the partial differential equation (11), over a local domain Ω_s bounded by Γ_s, can be obtained using the weighted residual method locally

$$\int_{\Omega_s} w_i(\sigma_{ij,j} + b_i - m\ddot{u}_i - c\dot{u}_i)\mathrm{d}\Omega - \alpha\int_{\Gamma_u} w_i(u_i - \bar{u}_i)\mathrm{d}\Gamma = 0 \tag{28}$$

The third term on the left hand side of equation (28) can be integrated by parts, and imposed the natural boundary condition (12a), we obtain:

$$\begin{aligned}\int_{\Omega_s}(w_i m\ddot{u}_i + w_i c\dot{u}_i + w_{i,j}\sigma_{ij})\mathrm{d}x - \int_{\Gamma_{si}} w_i t_i \mathrm{d}\Gamma - \int_{\Gamma_{su}} w_i t_i \mathrm{d}\Gamma + \alpha\int_{\Gamma_{su}} w_i u_i \mathrm{d}\Gamma \\ = \int_{\Gamma_{st}} w_i \bar{t}_i \mathrm{d}\Gamma + \alpha\int_{\Gamma_{su}} w_i \bar{u}_i \mathrm{d}\Gamma + \int_{\Omega_s} w_i b_i \mathrm{d}\Omega\end{aligned} \tag{29}$$

In the forced vibration analysis, **u** is the function both of space co-ordinate and time. Only space domain is discretized. Equations (5) can be re-written as

$$u^h(\mathbf{x},t) = \sum_{i=1}^{n} \phi_i(\mathbf{x}) u_i(t) \tag{30}$$

Substituting equations (30) into the local weak form (29) for all nodes leads to the following discrete equations

$$\mathbf{M}\ddot{\mathbf{u}}(t) + \mathbf{C}\dot{\mathbf{u}}(t) + \mathbf{K}\mathbf{u}(t) = \mathbf{f}(t) \tag{31}$$

where the mass matrix **M** is given by equation (20b), **K**, **C** and **f** are defined as

$$\mathbf{K}_{ij} = \int_{\Omega_s} \mathbf{v}_i^{\mathrm{T}} \mathbf{D}\mathbf{B}_j \mathrm{d}\Omega - \int_{\Gamma_{si}} \mathbf{w}_i \mathbf{N}\mathbf{D}\mathbf{B}_j \mathrm{d}\Gamma - \int_{\Gamma_{su}} \mathbf{w}_i \mathbf{N}\mathbf{D}\mathbf{B}_j \mathrm{d}\Gamma + \alpha\int_{\Gamma_{su}} \mathbf{w}_i \mathbf{\Phi}_j d\Gamma \tag{32a}$$

$$\mathbf{C}_{ij} = \int_{\Omega_s} c\mathbf{w}_i \mathbf{\Phi}_j \mathrm{d}\Omega \tag{32b}$$

$$\mathbf{f}_i(t) = \int_{\Gamma_{st}} \mathbf{w}_i \bar{\mathbf{t}}(t)\mathrm{d}\Gamma + \alpha\int_{\Gamma_{su}} \mathbf{w}_i \bar{\mathbf{u}}\mathrm{d}\Gamma + \int_{\Omega_s} \mathbf{w}_i \mathbf{b}(t)\mathrm{d}\Omega \tag{32c}$$

5.2 Direct analysis of forced vibration

The methods of solving equation (31) can be largely divided into two categories: the modal analysis and the direct analysis. The direct analysis methods are utilized in this paper. Several direct analysis methods have been developed to solve the dynamic

equation (31), such as central difference method and Newmark method (see, eg., Petyt, 1990). The central difference and Newmark methods are used in this paper.

(a) The central Difference Method

The central difference method (CDM) consists of expressing the velocity and acceleration at time t in terms of the displacement at time t-Δt, t and t+Δt using central finite difference formulation:

$$\ddot{\mathbf{u}}(t) = \frac{1}{\Delta t^2}(\mathbf{u}(t-\Delta t) - 2\mathbf{u}(t) + \mathbf{u}(t+\Delta t)) \tag{33a}$$

$$\dot{\mathbf{u}}(t) = \frac{1}{2\Delta t}(-\mathbf{u}(t-\Delta t) + \mathbf{u}(t+\Delta t)) \tag{33b}$$

where Δt is time step. The response at time t+Δt is obtained by evaluating the equation of motion at time t. The Central Difference Method is, therefore, an explicit method.

The CDM is conditionally stable. The stable critical time step for CDM can be obtained from the maximum frequencies based on the dispersion relation using (Belytschko et al., 2000)

$$\Delta t^{\text{crit}} = \max_i \frac{2}{\omega_i}(\sqrt{\xi_i^2 + 1} - \xi_i) \tag{34}$$

where ω_i is the frequency and ξ_i the fraction of critical damping in this mode. For non-uniform arrangements of the nodes, the critical time step can be obtained by the eigenvalue inequality.

$$\Delta t^{\text{crit}} = \min \frac{2}{(\max_Q \lambda_{\max}^Q)^{1/2}} \tag{35}$$

where $\lambda_{\max}^Q$ is the maximum eigenvalue at the quadrature point $\mathbf{x}_Q$. The value of $\lambda_{\max}^Q$ depends on the size of local integration cell and the size of the interpolation domain (Belytschko et al., 2000).

(b) The Newmark method

The Newmark method is a generalization of the linear acceleration method. This latter method assumes that the acceleration varies linearly within the interval (t, $t+\Delta t$). This gives

$$\ddot{\mathbf{u}} = \ddot{\mathbf{u}}_t + \frac{1}{\Delta t}(\ddot{\mathbf{u}}_{t+\Delta t} - \ddot{\mathbf{u}}_t)\tau \tag{36}$$

and

$$\dot{\mathbf{u}}_{t+\Delta t} = \dot{\mathbf{u}}_t + [(1-\delta)\ddot{\mathbf{u}}_t + \delta\ddot{\mathbf{u}}_{t+\Delta t}]\Delta t \tag{37a}$$

$$\mathbf{u}_{t+\Delta t} = \mathbf{u}_t + \dot{\mathbf{u}}\Delta t + [(\frac{1}{2}-\beta)\ddot{\mathbf{u}}_t + \beta\ddot{\mathbf{u}}_{t+\Delta t}]\Delta t^2 \tag{37b}$$

The response at time $t+\Delta t$ is obtained by evaluating the equation of motion at time $t+\Delta t$. The Newmark method is, therefore, an implicit method.

The Newmark method is a unconditionally stable provided

$$\delta \geq 0.5 \quad \text{and} \quad \beta \geq \frac{1}{4}(\delta + 0.5)^2 \tag{38}$$

One can find that $\delta = 0.5$ and $\beta = 0.25$ leads to acceptable results for most of problems. $\delta = 0.5$ and $\beta = 0.25$ are always used in this paper for simplification.

5.3 Numerical results

The forced vibration for a 2-D structures, a cantilever beam, as shown in Figure 7, is analyzed. The problem is solved for the plane stress case with E=3×10^7, ν=0.3 and thickness t=1.0. In this numerical example for the forced vibration analysis, the beam subjected to a parabolic traction at the free end, P=1000$g(t)$. $g(t)$ is the function of time. As shown in Figure 7 (b), 55 uniformed nodes are used to discretize the problem domain. For simplification, m=1.0 is considered and the units are taken as standard international (SI) units. Displacements and stresses for all nodes are obtained. Detailed results of

vertical displacement, u_y, on the middle node, A, of the free end of the beam are presented. For comparison, solutions for this problem are also obtained using the Finite Element software, ABAQUS/ Explicit.

a. Simple harmonic loading

Consider first $g(t) = \sin(\omega_f t)$, where ω_f is the frequency of the dynamic load. ω_f=27 is used in this example. The parameter, α in equation (27), on the performance of the method is firstly investigated.

The results of α=0.5, 1.0, 1.5 and 2.0 are obtained. The displacements u_y of point A are plotted in Figures 8 and 9. From these figures, one can observe that results will be unstable for both CDM and Newmark method when $\alpha \le 1.0$. Increase α is useful to increase the accuracy and the stability for both CDM and Newmark method. However, if the integration domain is too large (α too big), more sub-cells are needed to obtain accurate integrations. It will be computationally more expensive. Our study has found that $\alpha = 1.5 \sim 2.5$ works for most of problems. $\alpha = 1.5$ is used in following calculations.

In order to investigate the property of two different direct time integration methods, CDM and Newmark method, results of different time steps are obtained and plotted in Figure 10. It can be found that for $\Delta t = 1\times10^{-4}$ both methods obtain results in very agreement with FEM. When $\Delta t \ge \Delta t^{crit}$ (from equation 35, $\Delta t^{crit} \approx 1\times10^{-3}$), CDM will become unstable. However, the Newmark method is always stable for any time step. It demonstrated that the CDM is a conditionally stable method and the Newmark method is an unconditional stable method. A bigger time step can be used in Newmark method. Even Δt=1×10^{-3} or 1×10^{-2} is used, very good results can be obtained using Newmark

method. However, it should be noted that the computational error would increase with the increase of time step in the Newmark method. The accuracy of Newmark method would become unacceptable when the time step is too big (e.g. $\Delta t = 5\times10^{-2}$). The unconditional stable property of Newmark is very useful for the structural forced vibration analysis in engineering applications, especially when responses for a longer time are needed. A big time step can be used in the Newmark method, thus considerable computations can be saved.

Many time steps are calculated to check the stability of the presented MLPG formulation. Newmark method with $\Delta t = 5\times10^{-3}$ is used, and the damping coefficient, c=0.4, is considered. Results until to 20s (about 100 natural vibration periods) are plotted in Figure 11. It can be found that a very stable result is obtained. After a long period time, the forced vibration under a simple harmonic dynamic loading becomes a stable vibration with the forced frequency ω_f. From the vibration theory (Meirovitch 1980), a resonance will occur when the $\omega_f = \omega_i$, where ω_i is the i-th natural frequency. From Figure 11, one can observe that the amplitude of vibration is very big (i.e. about 15 times of static displacement) because of $\omega_f \approx \omega_1$. In addition, a beat vibration with the period T_b occurs when $\omega_f \approx \omega_1$. T_b can be obtained from Figure 11, T_b≈4.3. From the vibration theory, $T_b = \dfrac{2\pi}{|\omega_f - \omega_1|}$, the first natural frequency of the system can be computed out $\omega_1 = 28.3$, which is nearly same as the result obtained in the free vibration analysis by FEM, $\omega_1^{FEM} = 28$.

b. Transient loading

The transient response of the beam subjected to a suddenly loaded and suddenly vanished force P=1000$g(t)$ is considered. The function $g(t)$ is shown in Figure 12. The present MLPG method is used to obtain the transient response with and without damping. The Newmark method is utilized in this analysis. The result for c=0 is plotted in Figure 13. For comparison, the result obtained by the Finite Element software, ABAQUS/ Explicit, is shown in the same figure. Results obtained by the present MLPG method are in very good agreement with those obtained using FEM. Many time steps are calculated to check the stability of the presented MLPG formulation. The result for c=0.4 is plotted in Figure 14. From Figure 14, one can observe that the response is declined with time because of damping. A very stable result is obtained again.

6. Discussion and conclusions

MLPG formulations for free vibration and forced vibration analyses of two-dimensional solids and structures have been presented in this paper. Local weak forms are developed from the dynamic partial differential equation. The MLS approximation is used to obtain the shape functions. The present method is a truly meshless method, which does not need any "element" or "mesh" for both field interpolation and background integration.

Some important parameters on the performance of the method have been investigated. It has been found that the parameter α, which decides the size of the sub-domain needs to be chosen carefully, especially, in the dynamic analyses. It can be found that $\alpha = 1.5 \sim 2.5$ leads to acceptable results for most of problems.

Programs of the present MLPG method have been developed, and a number of numerical examples of free vibration and forced vibration analyses are presented to

demonstrate the validity and efficiency of the present method. The results presented are encouraging. It is demonstrated that the present method is easy to implement, and very flexible for free vibration and forced vibration analyses in solids and structures.

Reference

Atluri SN, **Cho JY**, **Kim HG**(1999a) Analysis of thin beams, using the meshless local Petrov-Galerkin (MLPG) method, with generalized moving least squares interpolation.Computational Mechanics 24: 334-347

Atluri SN, **Kim HG, Cho JY**(1999b) A critical assessment of the truly meshless local Petrov-Galerkin (MLPG), and Local Boundary Integral Equation (LBIE) methods. Computational Mechanics 24:348-372

Atluri SN, Zhu T (1998) A new meshless local Petrov-Galerkin (MLPG) approach in computational mechanics. Computational Mechanics 22:117-127.

Atluri SN, Zhu T(2000a) New concepts in meshless methods. Int. J. Numer. Methods Engrg. 47 (2000) 537-556.

Atluri SN, Zhu T (2000b) The meshless local Petrov-Galerkin (MLPG) approach for solving problems in elsto-statics. Computational Mechanics 225:169-179

Belytschko T, **Lu YY**, **Gu L** (1994) Element-Free Galerkin methods. Int. J. Numer. Methods Engrg. 37:229-256

Belytschko T, **Organ D** (1995) Coupled finite element-element–free Galerkin method. Computational Mechanics 17:186-195

Belytschko T, Guo Y, Liu WK and **Xiao SP(**2000) A unified stability of meshless particle methods. Int. J. Numer. Methods Engng. 48,1359-1400.

Brebbia CA, **Telles JC**, **Wrobel LC** (1984) Boundary Element Techniques. Springer Verlag, Berlin

Chati MK, Mukherjee S (2000) The boundary node method for three-dimensional problems in potential theory. Int. J. Numer. Methods Engrg.47,1523-1547.

Dolbow J, Belytschko T (1999) Numerical itegration of the Galerkin weak form in meshfree methods. Computational Mechanics 23: 219-230

Gu YT, Liu GR (2000a) A boundary point interpolation method for stress analysis of solids. submitted.

Gu YT, **Liu GR** (2000b) A coupled element free Galerkin/ boundary element method for stress analysis of two-dimensional solids. Comput. Methods Appl. Mech. Engrg. 191 (in press).

Lancaster P, **Salkauskas K** (1981) Surfaces generated by moving least squares methods. Math. Comput. 37, 141-158.

Liu GR (1999) A Point Assembly Method for Stress Analysis for Solid. In: Shim VPW(ed) Impact Response of Materials & Structures. Oxford, pp 475-480

Liu GR, **Gu YT** (2000a) Coupling Element Free Galerkin and Hybrid Boundary Element methods using modified variational formulation. Australasian Issue of Computational Mechanics 26: 166-173

Liu GR , **Gu YT** (2000b) A Local Point Interpolation Method for stress analysis of two-dimensional solids. Int. J. Structural Engineering and Mechanics (in press)

Liu GR, **Gu YT** (2001) A Point Interpolation Method for two-dimensional solid. Int. Journal for Numerical Methods in Eng. 50 (in press)**.**

Liu GR, Yan L (1999) A study on numerical integration in element free methods. Proceedings of Fourth Asia-Pacific Conference on computational Mechanics, Singapore, 979-984.

Liu GR, **Yan L** (2000) A Modified Meshless Local Petrov-Galerkin Method for Solid Mechanics Advances in Computational Engineering & Sciences, Los Angles, August, 1374-1379.

Liu WK, **Jun S, Zhang YF**(1995) Reproducing kernel particle methods. Int. J. Numer. Methods Engrg. 20: 1081-1106.

Meirovitch L (1980) Computational Methods in Structural Dynamics. Sijthoff & Noordhoff: Grningen.

Mukherjee YX, Mukherjee S (1997) Boundary node method for potential problems. Int. J. Num. Methods in Engrg. 40: 797-815.

Nayroles B, Touzot G, Villon P (1992) Generalizing the finite element method: diffuse approximation and diffuse elements. Comput. Mech. 10: 307-318.

Nagashima T (1999). Node-by node meshless approach and its application to structural analyses. Int. J. Numer. Methods Engng 46,341-385.

Ouatouati AEL, Johnson DA (1999) A new approach for numerical modal analysis using the element-free method. Int. J. Numer. Methods Engng. 46,1-27.

Petyt M (1990) Introduction to finite element vibration analysis. Cambridge University Press, Cambridge.

Strang G (1976) Linear Algebra and its application. Academic Press: New York

Zhu T, Zhang JD, Atluri SN (1998) A local boundary integral equation (LBIE) method in computational mechanics, and a meshless discretization approach. Computational Mechanics 21:223-235

Table 1 Natural frequency of a cantilever beam with different nodal distribution

Mode	Coarse node distribution			Fine node distribution		
	MLPG	**Nagashima (1999)**	**FEM (ABAQUS)**	**MLPG**	**Nagashima (1999)**	**FEM (ABAQUS)**
1	919.47	926.10	870	824.44	844.19	830
2	5732.42	5484.11	5199	5070.32	5051.21	4979
3	12983.25	12831.88	12830	12894.73	12827.60	12826
4	14808.64	14201.32	13640	13188.12	13258.21	13111
5	26681.81	25290.04	24685	24044.43	23992.82	23818
6	38961.74	37350.18	37477	36596.15	36432.15	36308
7	40216.58	38320.59	38378	38723.90	38436.43	38436
8	55060.24	50818.64	51322	50389.01	49937.19	49958
9	64738.59	63283.70	63584	64413.89	63901.16	63917
10	68681.87	63994.48	65731	64937.83	64085.90	64348

Unit: Hz

Table 2 Natural frequencies of a cantilever beam with different slenderness

Modes	*r*/*L*=0.144			*r*/*L*=0.029		
	MLPG	FEM (ABAQUS)	Euler beam	MLPG	FEM (ABAQUS)	Euler beam
1	3565.81	3546.1	4138.23	824.44	830.19	827.65
Error with Euler beam(%)	-13.83	-14.31	/	-0.39	0.31	/
2	13025.06	12864	25933.86	5070.32	4979	5186.77
Error with Euler beam(%)	18.56	20.6	/	-2.24	-4.01	/

Unit: Hz

Gu and Liu : Table 1 & 2

Table 3 Natural frequencies of a variable cross-section cantilever beam

Modes	ω(*rd/s*)				
	1	2	3	4	5
MLPG method	263.21	923.03	953.45	1855.14	2589.78
FEM (ABAQUS)	262.09	918.93	951.86	1850.92	2578.63

Table 4 Natural frequencies of a shear wall

Mode	*ω*(rd/s)		
	MLPG method	FEM (ABAQUS)	Brabbia et al.(1984)
1	2.069	2.073	2.079
2	7.154	7.096	7.181
3	7.742	7.625	7.644
4	12.163	11.938	11.833
5	15.587	15.341	15.947
6	18.731	18.345	18.644
7	20.573	19.876	20.268
8	23.081	22.210	22.765

Gu and Liu : Table 3 & 4

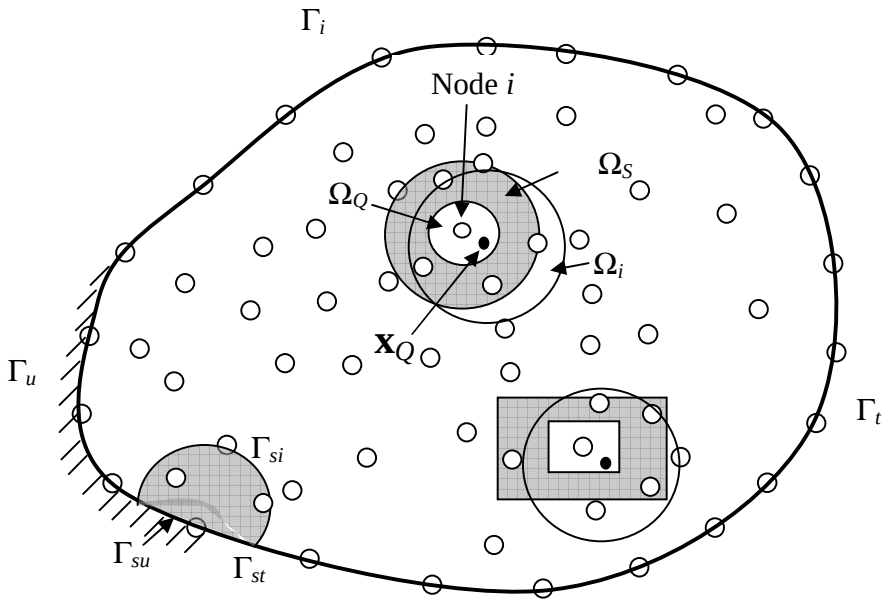

Fig. 1 The support domain Ω_S and integration domain Ω_Q for node i; the interpolation domain Ω_i for Gauss integration point $\mathbf{x}_Q$

Gu and Liu : Fig. 1

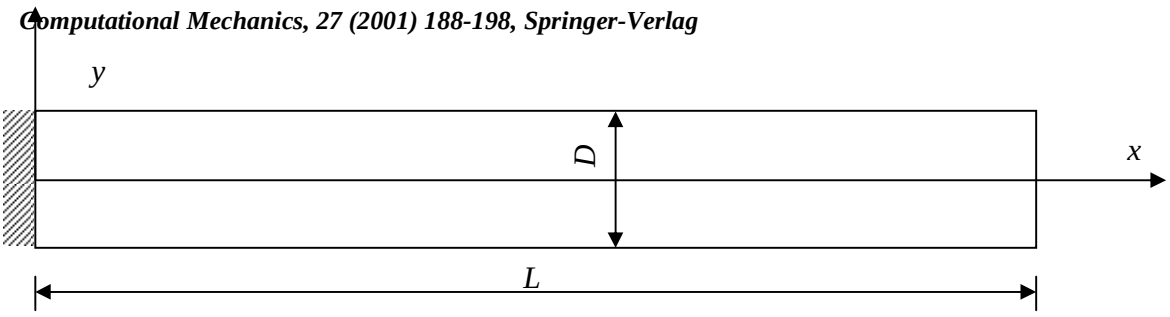

Fig 2. Cantilever beam

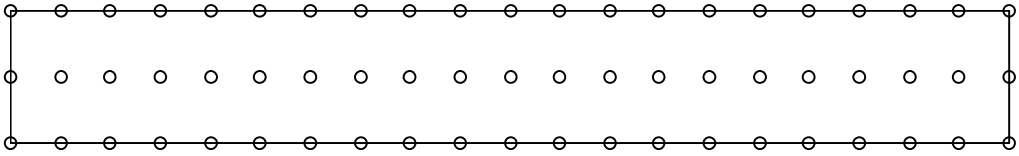

Fig 3(a). Coarse nodal distribution

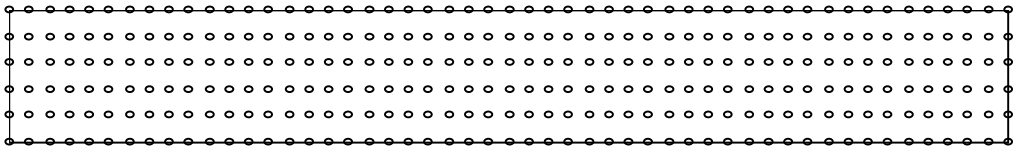

Fig. 3(b) Fine nodal distribution

Gu and Liu : Fig. 2 & 3

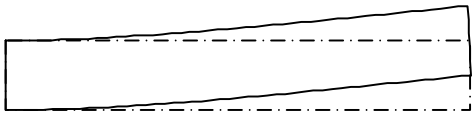

Mode 1

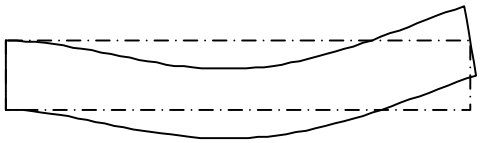

Mode 2

Mode 3

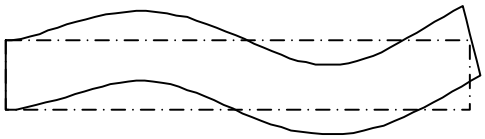

Mode 4

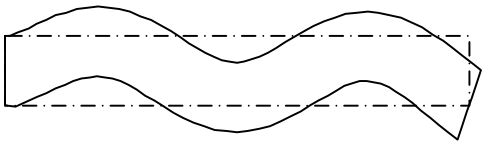

Mode 5

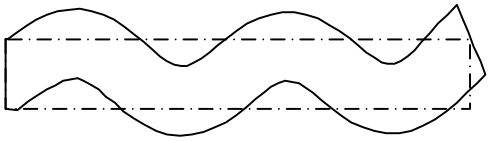

Mode 6

Gu and Liu : Fig. 4

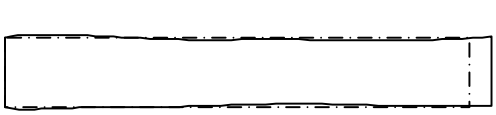

Mode 7

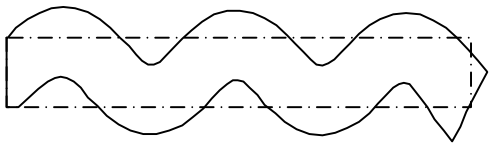

Mode 8

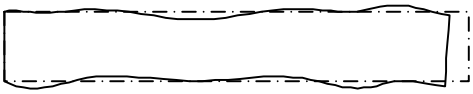

Mode 9

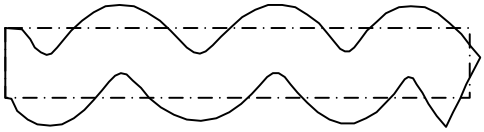

Mode 10

Fig. 4 Eigenmodes for the cantilever beam by MLPG method

Gu and Liu : Fig. 4

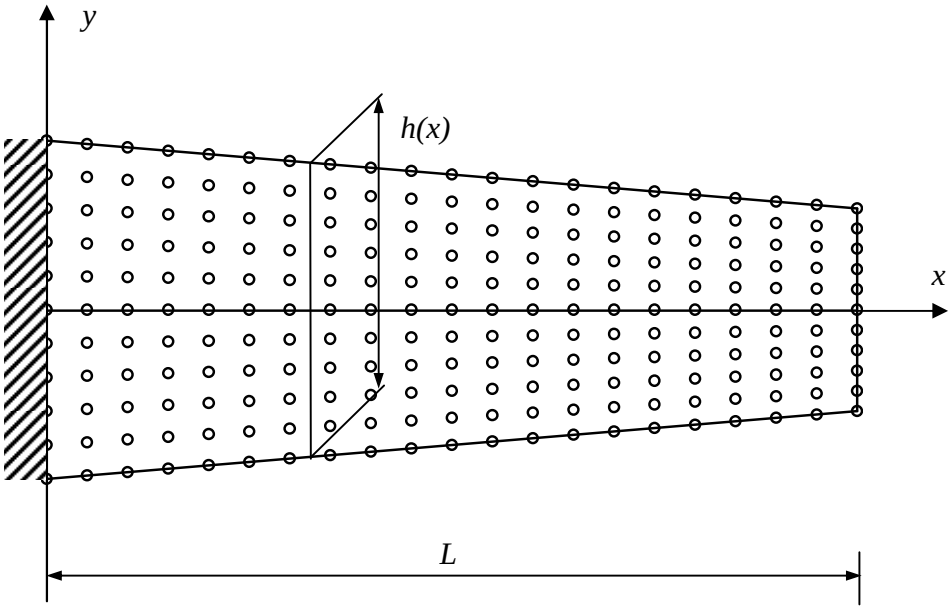

Fig. 5 A cantilever beam with variable cross-section

Gu and Liu : Fig. 5

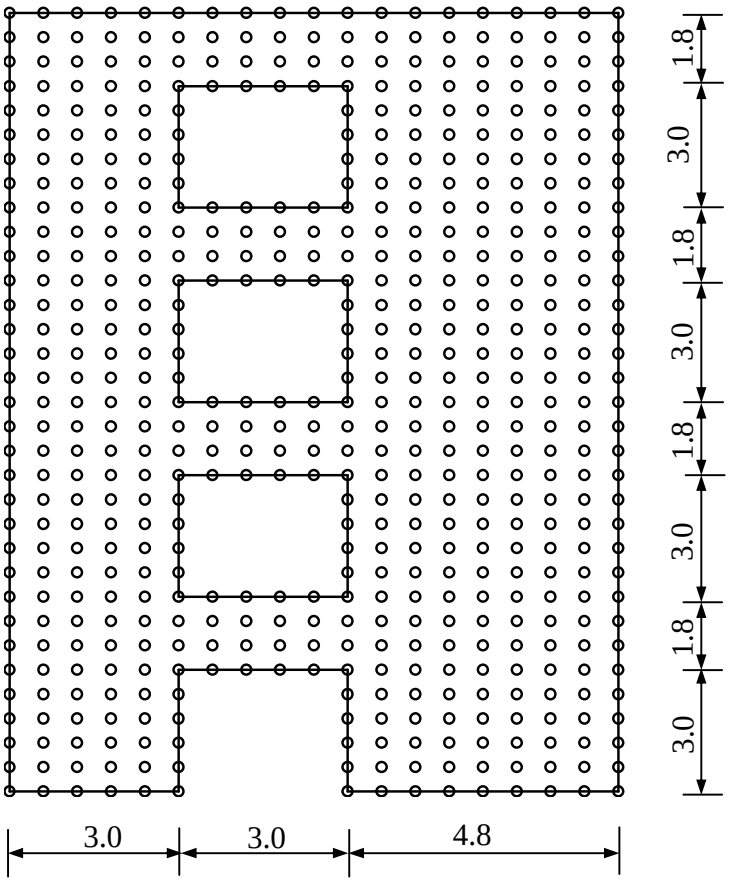

Fig. 6 A Shear wall with four openings

Gu and Liu : Fig. 6

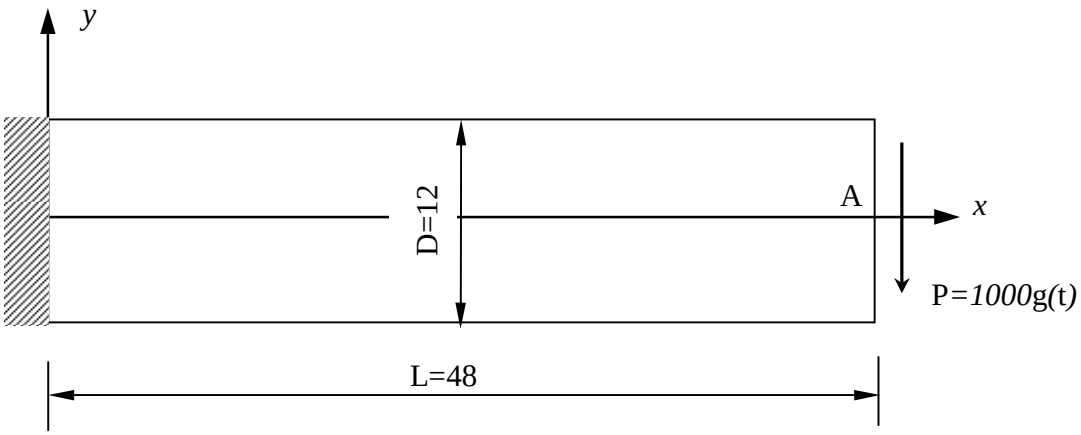

Fig. 7 (a) A Cantilever beam subjected a parabolic

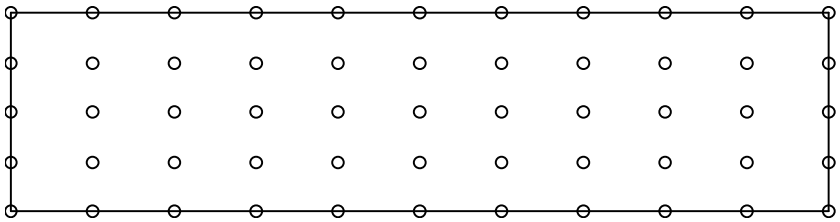

Fig. 7 (b) The nodal arrangement

Gu and Liu : Fig. 7

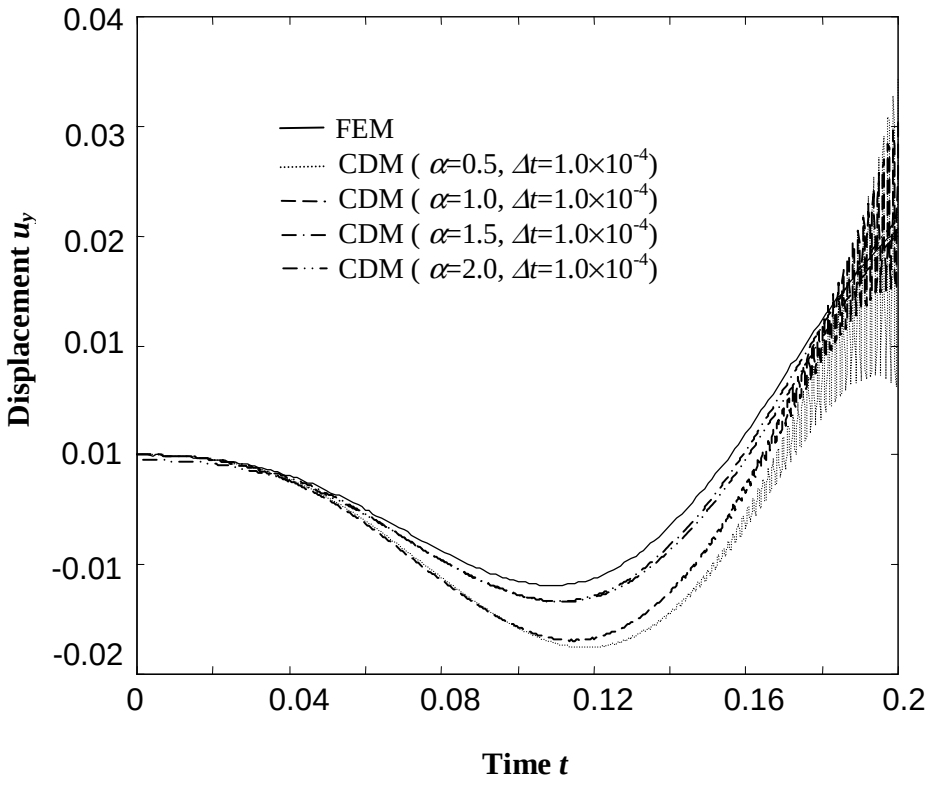

Fig. 8 Displacements u_y at point A using Central Difference Method (CDM) ($g(t)=\sin(\omega t)$)

Gu and Liu : Fig. 8

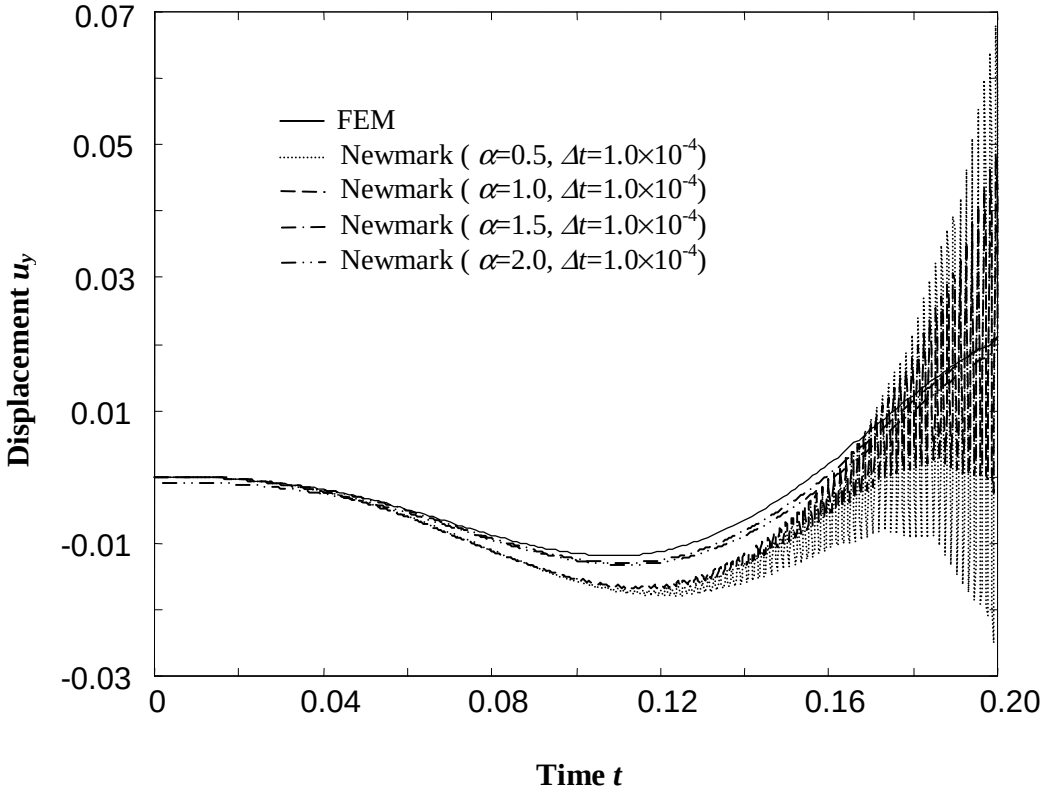

Fig. 9 Displacements u_y at point A using Newmark method ($\delta = 0.5$ and $\beta = 0.25$, with $g(t)=\sin(\omega t)$)

Gu and Liu : Fig. 9

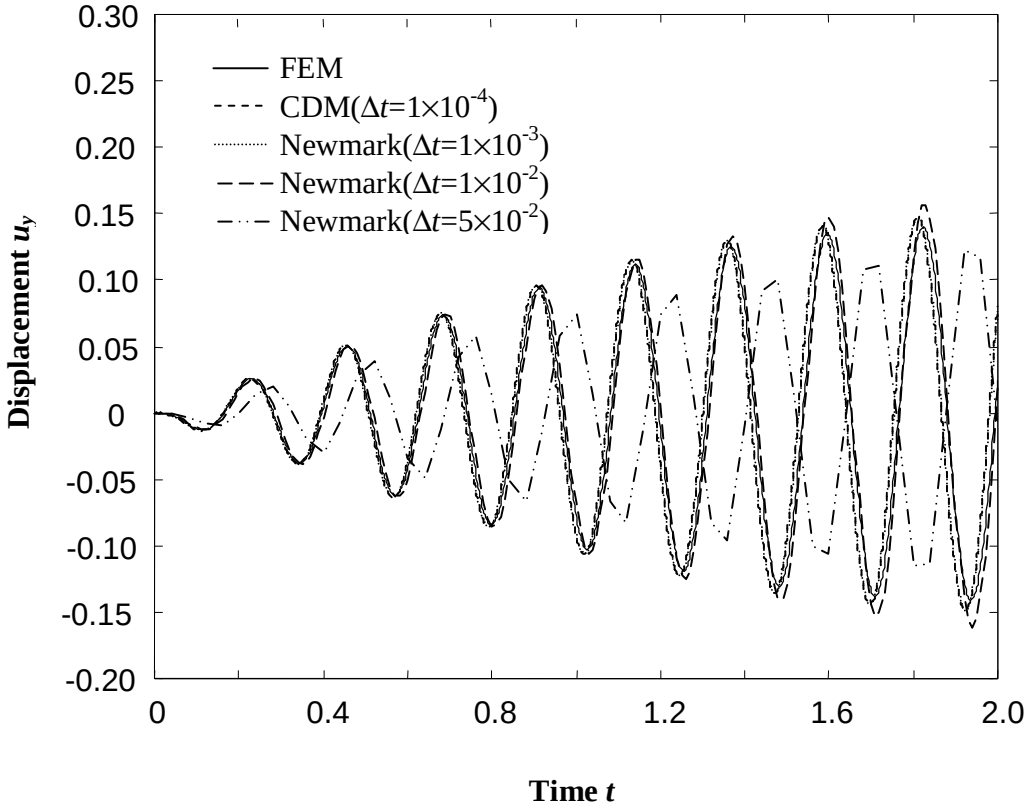

Fig. 10 Displacements u_y at the point A ($g(t)=\sin(\omega t)$)

Gu and Liu : Fig. 10

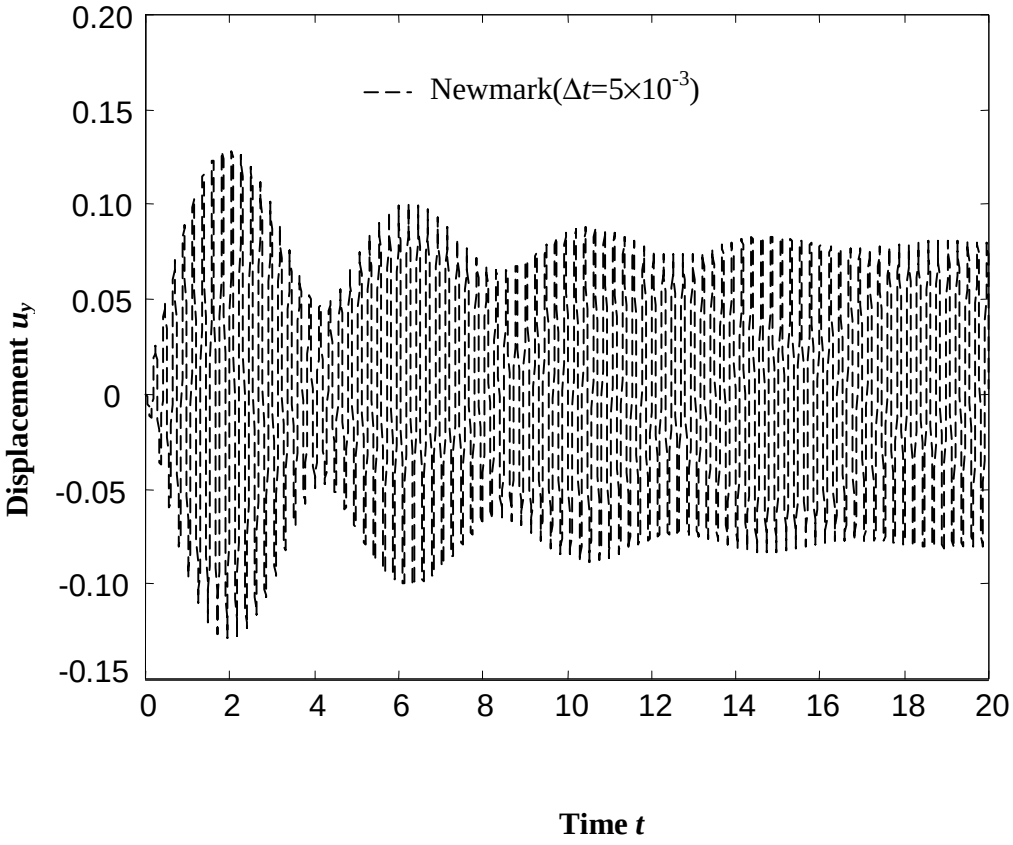

Fig. 11 Displacements u_y at point A ($g(t)=\sin(\omega t)$)

Gu and Liu : Fig. 11

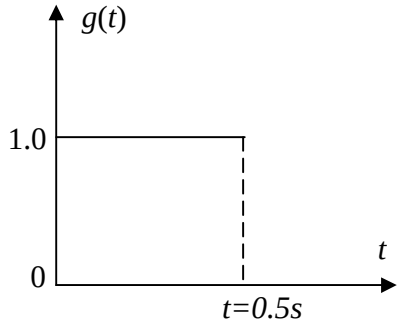

Fig. 12 The function *g*(*t*)

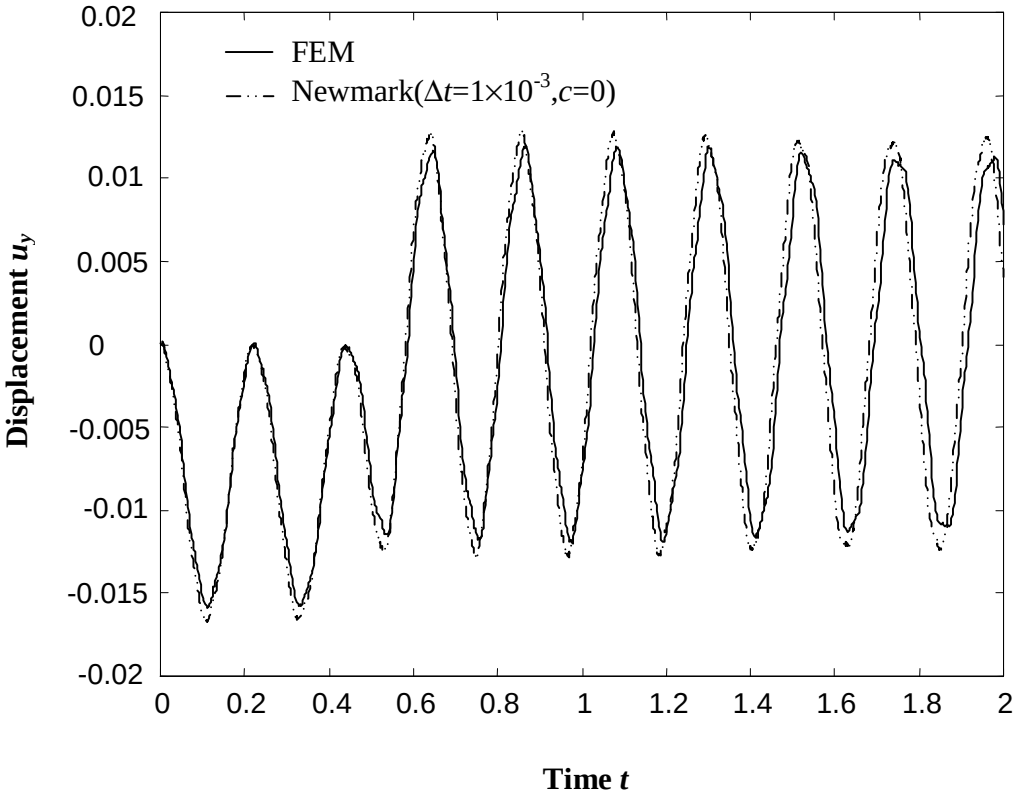

Fig. 13 Transient displacements u_y at point A using Newmark method ($\delta = 0.5$ and $\beta = 0.25$)

Gu and Liu : Fig. 12 & 13

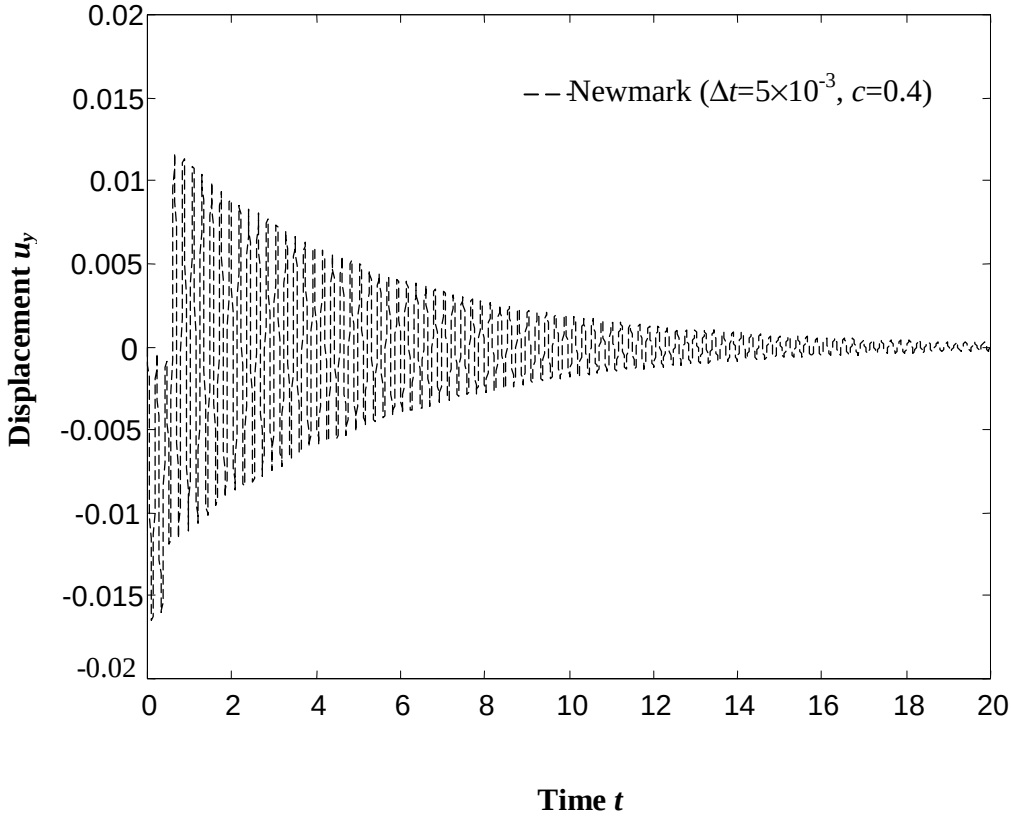

Fig. 14 Transient displacements u_y at point A using Newmark method ($\delta = 0.5$ and $\beta = 0.25$)

Gu and Liu : Fig. 14